Direct numerical evaluation of earth return path impedances of underground cables

G.K. Papagiannis, D.A. Tsiamitros, D.P. Labridis and P.S. Dokopoulos

Abstract: The lossy earth return path influences significantly the impedances of underground power cables, especially in cases where transient simulation models are of interest. The use of approximations for the calculation of the earth correction terms proves to be inaccurate, especially at high frequencies or for low earth resistivities. A novel direct numerical integration scheme for the evaluation of the infinite integral terms is presented. The new method proves to be numerically stable and efficient in all cases examined. Results obtained by the novel integration scheme are compared with those obtained by other approaches, as well as by a finite-element method formulation for several single-core cable configurations and for cases of homogeneous and multilayered earth.

1 Introduction

In transient simulations, detailed transmission line modelling is required. In the case of underground power cables, the model parameters are strongly influenced by the resistive earth return path. The influence of the lossy earth on conductor impedances has been analysed since 1926. For the case of overhead lines, correction terms can be calculated using the widely accepted Carson's formulas [1]. Similar formulas have been developed by Pollaczek [2], applicable not only to overhead conductors but also to cases of underground isolated conductor systems and to combinations of both. In these approaches earth is assumed to be homogeneous and semi-infinite.

Both approaches lead to complicated expressions with complex infinite integrals. These integrals have been approximated using algebraic infinite series. This evaluation has been adopted by Wedepohl and Wilcox [3] and by Ametani [4], who proposed general models for the simulation of wave propagation in power cables. The formulation of [4] was also adopted in the Cable constants/parameters supporting routines of the well-known Electromagnetic Transients Program (EMTP) [5].

The electromagnetic field of current-carrying conductors results from the conductors and their images. For underground cables, however, the earth contribution is much more significant as the actual conductors are in the ground and their images in the air. This leads to infinite integrals for the self and mutual earth return impedances, which differ from the corresponding ones for overhead lines. They include highly oscillatory functions and therefore are not easy to evaluate numerically. To overcome these difficulties several approaches have been proposed. Besides infinite series approximations, a simplified closed-form approximation has been proposed in [6], while direct numerical integration is used in [7], but certain numerical problems, limiting the efficiency of the method, are reported. In a recent approach [8] the difficulties related to the specific form of the integral terms are once again reported and an integration algorithm is proposed for complementary use to the existing methodologies.

A further complication is due to the fact that the real ground is composed of several layers with different electromagnetic properties. Sunde [9] extended the homogeneous earth solution of [1, 2] and developed new formulas for the case of a two-layer earth under certain assumptions. The resulting integral forms for the case of underground conductors are very complex and were practically abandoned. In 1973, Nakagawa [10] proposed a more rigorous and general solution but only for the case of overhead conductors above a multilayered earth model. Therefore there is a lack in modelling cases of underground cables in non-homogeneous earth structures.

The finite-element method (FEM) is a numerical method widely used for the solution of electromagnetic field equations in a region, regardless of the geometric complexity. The application of FEM in cable parameter calculation was proposed in [11] mainly for pipe-type cables, where the discretisation area is limited inside the pipe. In a recently proposed method by some of the present authors [12], a suitable FEM formulation was used in the computation of overhead transmission-line parameters with unbounded discretisation areas. The method is capable of handling cases of terrain surface irregularities and non-homogeneous, stratified soil, where most classical methods usually fail.

This paper presents a novel numerical integration technique, which can be used for the direct calculation of the earth return impedances of underground cable arrangements for the case of homogeneous earth. The technique is based on proper combinations of numerical integration methods to overcome efficiently the problems arising from the oscillative form of the infinite integrals. Results obtained by the novel method are compared against those obtained by the EMTP supporting routines for several cable arrangements, earth resistivities and frequencies. The new method eliminates the need for approximations and shows remarkable numerical stability and efficiency.

IEE Proceedings online no. 20045011

doi:10.1049/ip-gtd:20045011

Paper first received 21st April 2004 and in revised form 3rd November 2004. Originally published online: 8th April 2005

The authors are with the Power Systems Laboratory, Department of Electrical & Computer Engineering, Aristotle University of Thessaloniki, P.O. Box 486, Thessaloniki GR-54124, Greece

E-mail: grigoris@eng.auth.gr

Finally a FEM formulation is used both for the justification of the results of the novel approach as well as for the evaluation of the complex impedances in cases of cable arrangements in two-layer earth structures. Certain cases of two-layer earth models, based on actual ground resistivity measurements, are investigated and the results are compared with those of the homogeneous earth case.

2 Earth return impedances of underground cable systems

A transmission line is generally described by the two matrix equations, which are shown in (1) and (2), linking the voltages and currents across the line:

$$\frac{\partial}{\partial z}\boldsymbol{v} = -\boldsymbol{Z}'(\omega)\boldsymbol{i} \tag{1}$$

$$\frac{\partial}{\partial z}\boldsymbol{i} = -\boldsymbol{Y}'(\omega)\boldsymbol{v} \tag{2}$$

where $\omega = 2\pi f$ is the angular velocity, $\boldsymbol{v}$ is the voltage vector with respect to a reference conductor, $\boldsymbol{i}$ is the current vector and $\boldsymbol{z}$ is the longitudinal direction along the transmission line. Matrices $\boldsymbol{Z}'(\omega)$ and $\boldsymbol{Y}'(\omega)$ are the frequency dependent series impedance and shunt admittance per unit length matrices, respectively.

For the case of an underground cable system, $\boldsymbol{Z}'(\omega)$ may be considered to consist of two components [4]:

$$\boldsymbol{Z}'(\omega) = \boldsymbol{Z}'_i(\omega) + \boldsymbol{Z}'_e(\omega) \tag{3}$$

where $\boldsymbol{Z}'_i(\omega)$ represents the internal impedances of the conductors in the cable system and $\boldsymbol{Z}'_e(\omega)$ accounts for the influence of the earth return path. The exact form and the dimensions of the above matrices depend on the number of conducting elements of each cable, e.g. core, sheath, armour, and on the type and the actual configuration of the cable system. In the case of single-core (SC) cables, the diagonal elements of $\boldsymbol{Z}'_e(\omega)$ represent the impedances of the loops formed by the outermost tubular conductor of the cables, either sheath or armour and the earth, while the non-diagonal elements account for the mutual impedances between the outermost tubular conductors of each pair of cables and the earth.

The cable arrangement of Fig. 1 consists of two SC cables i and j, buried in the ground, which is considered to be semi-infinite and homogeneous, having an earth resistivity ρ and relative permeability and permittivity of μ_r and ε_r, respectively.

According to [2, 3], the mutual earth return impedance between the two underground cables i and j is

$$\overline{\boldsymbol{Z}}'_{mutual} = \frac{\rho m^2}{2\pi}\left\{K_0(md) - K_0(mD) + \overline{J}_m\right\} \tag{4}$$

with

$$\overline{J}_m = \int_{-\infty}^{\infty} \frac{e^{-(h+y)\sqrt{a^2+m^2}}}{|a| + \sqrt{a^2+m^2}} e^{jax}\, da \tag{5}$$

$$D = \sqrt{x^2 + (h+y)^2},\ d = \sqrt{x^2 + (h-y)^2},$$
$$m = \sqrt{j\omega\mu_r\mu_0/\rho}$$

where j is the imaginary unit, μ_0 is the free space permeability and K_0 is the modified complex Bessel function of the second kind with zero order. The integral form of (5) results from the application of the Fourier integral transform on the generalised wave equations in the ground and in the air [13]. The parameter a in (5) is the transformed space variable and mathematically represents the frequency of the Fourier spectrum [14]. The self-impedance formula is derived from (4) and (5) by putting $x = r$ and $y = h$, where r is the radius of the outermost surface of the cable.

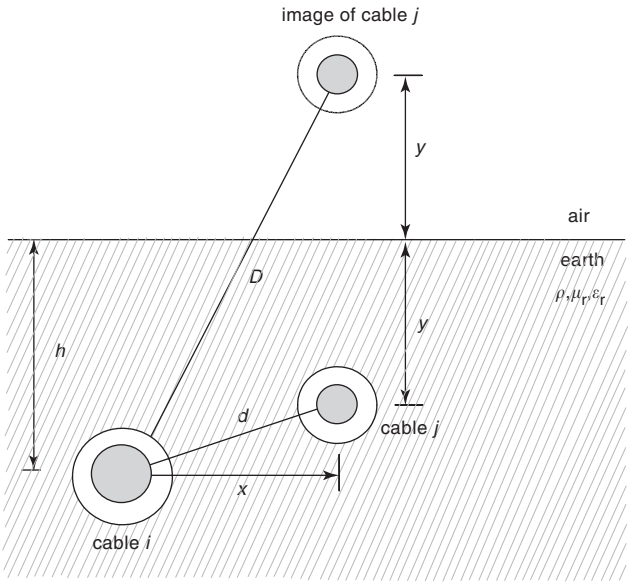

Fig. 1 *Geometric configuration of two single-core underground cables*

By applying some simple transformations in (5) the following relation results [9]:

$$\overline{J}_m = 2\int_0^{\infty} \frac{e^{-(h+y)\sqrt{a^2+m^2}}}{a + \sqrt{a^2+m^2}} \cos(xa)\, da \tag{6}$$

3 Numerical evaluation of the infinite integral

The corresponding expression for the mutual earth return impedances of conductors above ground is [1]:

$$\overline{Z}'_m = \frac{\rho m^2}{2\pi}\ln\left(\frac{D}{d}\right) + \overline{J}'_m \tag{7}$$

where

$$\overline{J}'_m = \frac{\rho m^2}{\pi}\int_0^{\infty} \frac{e^{-(h+y)a}}{a + \sqrt{a^2+m^2}} \cos(xa)\, da \tag{8}$$

The variables h, y, x, D and d of (7) and (8) correspond to the variables presented in Fig. 1, assuming that air and earth in Fig. 1 switch places. The relative permeability and permittivity in the air are considered to be equal to one. Thus m in (7) and (8) is $m = \sqrt{j\omega\mu_0/\rho}$.

Equations (4) and (7) differ mainly in two points. First (4) includes the Bessel functions instead of the natural logarithm term. However, these functions seem to present no serious problem as they can be evaluated easily using standard library functions. The key difference though is the fact that the exponential function in the infinite integral in (6) is complex, whereas in (8) it is real. As a result the real and imaginary parts of the infinite integral of (8) are monotonic and non-oscillatory functions [1] and can be calculated by infinite series, which converge rapidly [5].

In the approach of Wedepohl [3], the infinite integral of (5) is divided into parts, each of which is approximated using infinite series. Simplified expressions of the general

formulas are also proposed for low frequencies and common cable configurations.

In [5] it is recognised that the integral term in (5) becomes identical to Carson's earth return impedance if the numerator $e^{-(h+y)\sqrt{a^2+m^2}}$ is replaced by $e^{-(h+y)a}$. Accepting this approximation, which is valid for $|a| >> |m|$, Carson's infinite series or asymptotic expansion can be used for the numerical evaluation of (5). However this approximation is highly uncertain especially for high frequencies and for low earth resistivities. This drawback is reported in [5]. In the same reference a single case of two underground conductors is examined using the above approximation together with Wedepohl's approach [3]. The results are compared with those obtained by the numerical integration of (5), using the Romberg extrapolation [15]. The approximation of EMTP shows significant differences for frequencies greater than 10 kHz, while Wedepohl's approach is accurate enough at least up to 100 kHz. Numerical efficiency problems concerning the application of the integration method are also reported.

Direct numerical integration is also used in [7]. Several integration methods, such as the Simpson rule and Romberg rule, are tried. Problems concerning the numerical efficiency and the stability of these methods are reported, leading to the adaptation of artificial intelligence techniques for the evaluation of the infinite integrals.

Finally, in [8] the integral of (6) is transformed into a more convenient form and is then approximated by a finite one, according to a truncation criterion. To avoid numerical oscillations the finite integration range is separated into several sub ranges, which are calculated using the trapezoidal rule. The proposed technique is considered by the authors to be complementary to other methods.

Most of the above approaches either use approximations, which are valid only within certain limits, or suffer from numerical efficiency, which prohibits their generalised application. Therefore the problem of finding an efficient and accurate general-purpose method for the numerical evaluation of the infinite integral in (6) is still of research interest.

Direct numerical integration of the infinite integral is the method used in this paper for the evaluation of (6). Instead of using the previously mentioned integration algorithms, a novel integration technique has been developed, based on combinations of integration methods. More specifically, the Gauss–Legendre method [15], a highly accurate numerical integration method applicable in finite intervals of functions, is combined with two other numerical integration methods: the Gauss–Laguerre method [15], which is best suited for infinite integrals and the Lobatto rule, a very efficient numerical integration method for oscillative functions [15]. The selective implementation of the different numerical integration methods in the intervals between the roots of $\cos(ax)$, for both the real and the imaginary part of $\overline{J}_m$, leads to a quick and very efficient integration scheme for the evaluation of (6). An analytical description of the novel technique is presented in the Appendix.

4 Finite-element approach

The problem of the calculation of the cable series impedance matrix in (1) could be greatly simplified, assuming that the per unit length voltage drop $\overline{V}_i$ on every conductor is known for a specific current excitation. The mutual complex series impedance per unit length $\overline{Z}'_{ij}$ between conductor i and another conductor j carrying current $\overline{I}_j$, where all other conductors are forced to carry zero currents, is then given by:

$$\overline{Z}'_{ij} = \frac{\bar{V}_i}{\overline{I}_j} \quad (i, j = 1, 2, \ldots\ldots, n) \tag{9}$$

The self impedance of a conductor may also be calculated from (9), by setting $i=j$. In such a case, the following procedure may be used for the calculation of the cable series impedance matrix [12]:

- A sinusoidal current excitation of arbitrary magnitude is applied sequentially to each cable conductor, while the remaining conductors are forced to carry zero currents. The corresponding voltages are recorded.
- Using (9), the self and mutual impedances of the j cable conductor may be calculated. This procedure is repeated n times in order to calculate the impedances of n conductors.

Therefore, the problem is reduced to that of calculating the actual per unit length voltage drops, when a current excitation is applied to the conductors. This may be achieved by a suitable-FEM formulation of the electromagnetic diffusion equation.

An underground power cable arrangement, consisting of n parallel conductors, is assumed to be long enough to ignore end effects. Furthermore, if the current density vector is supposed to be in the z direction, the problem becomes two-dimensional and it is confined to the x–y plane, in which the conductors' cross-sections lie. The above two-dimensional diffusion problem is described by the system of equations [16]:

$$\frac{1}{\mu_0\mu_r}\left[\frac{\partial^2\overline{A}_z}{\partial x^2} + \frac{\partial^2\bar{A}_z}{\partial y^2}\right] - j\omega\sigma\overline{A}_z + \bar{J}_{sz} = 0 \tag{10}$$

$$-j\omega\sigma\overline{A}_z + \overline{J}_{sz} = \overline{J}_z \tag{11}$$

$$\int_{S_i}\int \overline{J}_z dS = \overline{I}_i, \quad i = 1, 2, \ldots, n \tag{12}$$

where $\overline{A}_z$ is the z direction component of the magnetic vector potential (MVP).

In (11) the total current density $\overline{J}_z$ is decomposed into two components:

$$\overline{J}_z = \overline{J}_{ez} + \overline{J}_{sz} \tag{13}$$

where $\overline{J}_{ez}$ is the eddy current density and $\overline{J}_{sz}$ is the source current density, given by:

$$\overline{J}_{ez} = -j\omega\sigma\overline{A}_z \tag{14}$$

$$\overline{J}_{sz} = -\sigma\nabla\Phi \tag{15}$$

FEM is applied for the solution of (10) and (11) with the boundary conditions of (12). Values for $\overline{J}_{sz_i}$ on each conductor i of conductivity σ_i are then obtained and (9) takes the form

$$\overline{Z}'_{ij} = \frac{\bar{V}_i}{\overline{I}_j} = \frac{\overline{J}_{sz_i}/\sigma_i}{\overline{I}_j}, \quad i, j = 1, 2, \ldots, n \tag{16}$$

linking properly electromagnetic field variables and equivalent circuit parameters.

The results obtained by FEM are highly accurate as they are obtained by solving the actual electromagnetic field equations of the system. A further distinct advantage of the FEM is its capability of handling cases of almost any kind of geometrical or electromagnetic irregularities of the ground, where conventional methods fail.

5 Numerical results

The proposed numerical integration scheme is applied in the following cases of SC cable arrangements in homogeneous ground. First the case of a shallowly located SC cable system of Fig. 2 is examined [11] in a horizontal (Fig. 2*a*) and a vertical (Fig. 2*b*) cable arrangement. The cable is at a depth $h = 1.2\,\text{m}$ with a spacing of $s = 0.25\,\text{m}$ in the horizontal arrangement. The core radius is $r_c = 23.4 \times 10^{-3}\,\text{m}$, while the outer radius is $r_s = 48.4 \times 10^{-3}\,\text{m}$. The conductance of the cable core is $\sigma = 5.88235 \times 10^7\,\text{S/m}$, while $\mu_r = 1$ and $\varepsilon_r = 1$ for all the media in Fig. 2. The conductivity of the air is considered to be zero.

Series impedances are calculated for this configuration using the proposed integration scheme and they are compared to the corresponding impedances obtained by the EMTP and the FEM methods. The earth resistivity is considered to vary from 2 up to 1000 Ωm and the frequency range examined is from 1 Hz to 10 MHz, to cover power system operating conditions from steady state up to very fast lightning surges. For each case the relative differences in the form of (17) are calculated:

$$\text{relative difference } (\%) = \frac{\left||\overline{Z}_{Num}| - |\overline{Z}_{EMTP}|\right|}{|\overline{Z}_{EMTP}|} \times 100 \quad (17)$$

Figure 3 shows the relative differences for the magnitude of the self impedance of the horizontal cable arrangement of Fig. 2. Differences up to 12% occur, especially for low earth resistivities and high frequencies.

Figure 4 shows the corresponding differences for the magnitude of the mutual impedance of the cable arrangement. The differences in this case are due only to the different approaches in earth return impedance calculation and are higher, reaching up to 30%.

Next the case of a SC cable with core and sheath, as in Fig. 5 is considered. Original cable data from [3] are reproduced in Table 1. The cable arrangements are similar to those in Fig. 2*b* with $h = 0.75\,\text{m}$, $s = 0.15\,\text{m}$ and $\mu_r = 1$ for all the media.

The differences of (17) are calculated for the above cable arrangement using the previous earth resistivities and frequencies. Figs. 6 and 7 show these differences for the case of the vertical configuration, for the real and the imaginary parts of the mutual impedance between the cable sheaths, respectively. Differences of almost 25% are recorded.

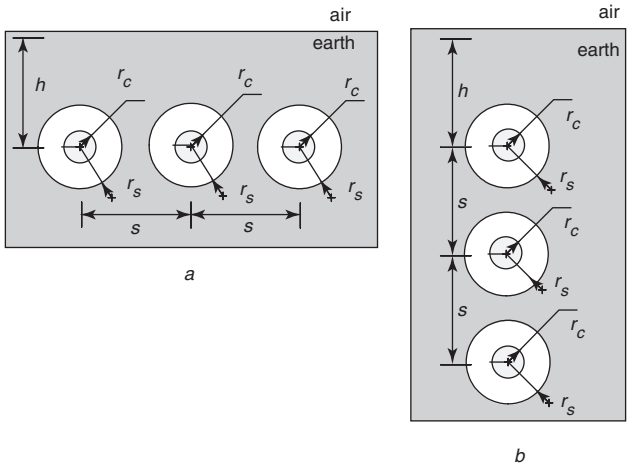

Fig. 2 *Single-core cable arrangements in homogeneous ground*
a Horizontal
b Vertical

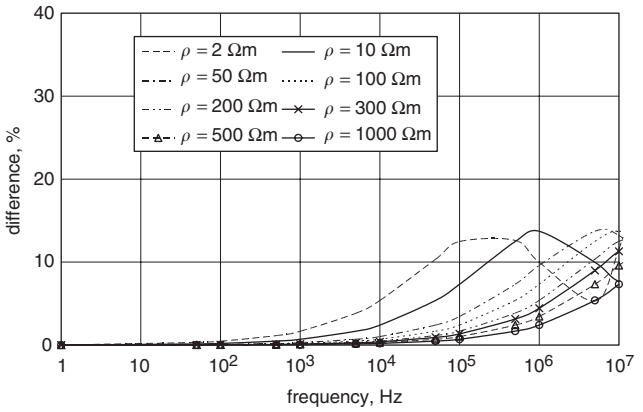

Fig. 3 *Differences in Z_{11} between numerical integration and EMTP*

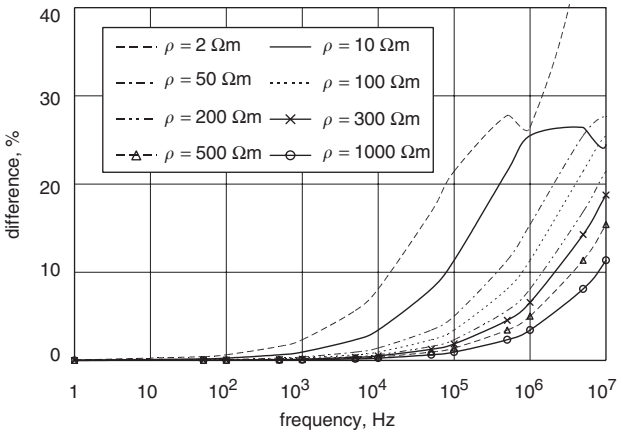

Fig. 4 *Differences in Z_{12} between numerical integration and EMTP*

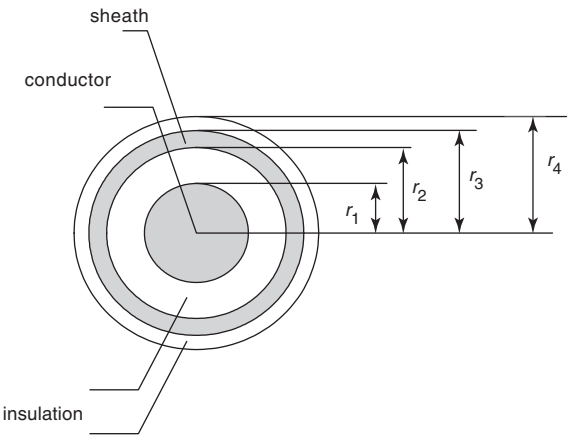

Fig. 5 *Single-core cable with core and sheath*

Table 1: Data of the SC cable arrangement of Fig. 5

Core radius r_1	0.0127 m
Main insulation radius r_2	0.0228 m
Sheath radius r_3	0.0254 m
Outer insulation radius r_4	0.0279 m
DC resistance of copper core	0.034 Ω/km
DC resistance of lead sheath	0.436 Ω/km

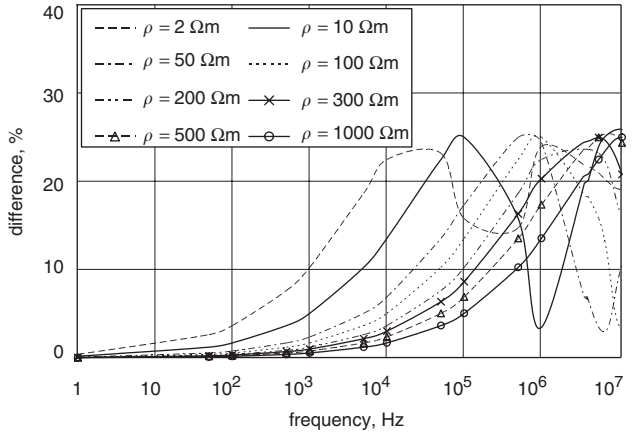

Fig. 6 *Real part of mutual impedance of cable sheaths; differences between numerical integration and EMTP*

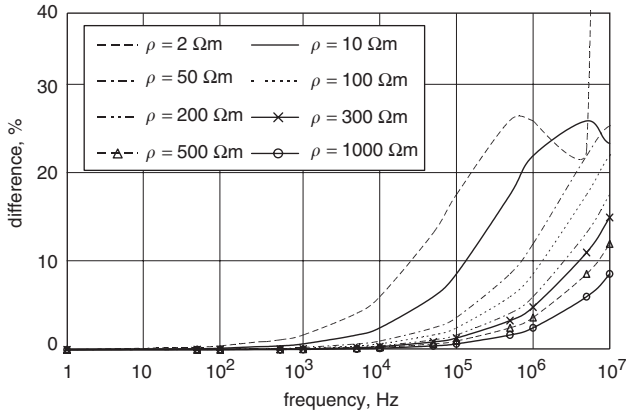

Fig. 7 *Imaginary part of mutual impedance of cable sheaths: differences between numerical integration and EMTP*

All results show that significant differences in the calculated earth return impedances occur, mainly for frequencies above 10 kHz. The differences are greater for low earth resistivities, reaching almost 30% and starting even at power frequency for the case of mutual impedances, where the influence of the earth is more distinct. This is because, under these conditions, the assumptions used in the EMTP calculation method are no longer valid. These differences can influence the behaviour of cable modelling in transient simulations and must be taken into account.

To justify the validity of the results of the direct numerical integration, they were checked against the corresponding by FEM for all above cases. The differences calculated by a formula similar to (17) are less than 1% for all cases over the whole range of frequencies and earth resistivities. In all cases examined the novel numerical integration scheme proved to be numerically stable. The computation time for the numerical integration is less than 5 s for a set of 280 earth resistivity and frequency combinations using an Intel Pentium IV PC running at 1.7 GHz.

The case of a multilayered earth is considered next. Sunde's extension for multilayered earth structures [9] refers only to conductors over or on the surface of the ground. For the case of underground conductors no solution for the electromagnetic field exists in the literature. Therefore the FEM is used for the calculation of the impedance matrices of cables buried in a two-layered earth. The horizontal arrangement of Fig. 2*a* is considered. Six different two-layered earth models were investigated, based on actual grounding parameter measurements [17]. The corresponding data for the resistivities ρ_1 for the first and ρ_2 for the second layer and for the depth d of the first layer are shown in Table 2. The second layer is of infinite extent.

Cable impedances were obtained by FEM for the frequency range 50 Hz–1 MHz, to cover conditions from steady state up to fast lightning transients. Results are compared against the corresponding ones obtained by the proposed numerical integration scheme, under the assumption of homogeneous earth. Differences calculated by a formula similar to (17) are shown in Fig. 8 concerning the magnitude of the mutual impedance between the cables in Fig. 2*a*. The homogeneous earth model is assumed to have resistivity ρ_1 of the first earth layer. Differences of up to 22% are encountered, especially in cases of great divergence between the resistivities of the two layers. Differences start at power frequency and are amplified at higher frequencies.

Another interesting feature is that these differences persist even at very high frequencies where the penetration depth, calculated by (18), approaches the depth of the first layer. For overhead lines over multilayered ground these differences disappear in such cases [18]. This is an indication that the validity of (18) for underground conductors must be further investigated:

$$p = \frac{1}{\sqrt{\pi f \mu_0 \sigma}} \tag{18}$$

This remark is also validated by the results in Fig. 9, where the differences for the magnitude of the self impedance are shown, as calculated by FEM and the numerical integration method, assuming homogeneous earth.

Table 2: Two-layered earth models

	ρ_1(Ωm)	ρ_2(Ωm)	d(m)
Case I	372.729	145.259	2.690
Case II	246.841	1058.79	2.139
Case III	57.344	96.714	1.651
Case IV	494.883	93.663	4.370
Case V	160.776	34.074	1.848
Case VI	125.526	1093.08	2.713

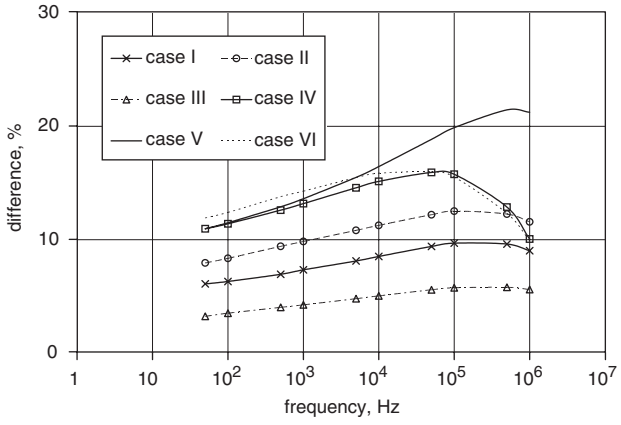

Fig. 8 *Two-layered earth case: differences in magnitude of mutual impedance*

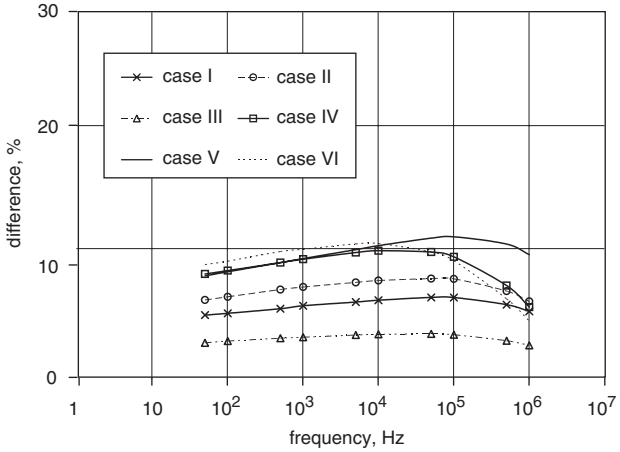

Fig. 9 *Two-layered earth case: differences in magnitude of self impedances*

6 Conclusions

This paper has addressed the problem of the calculation of the earth return impedances for simulating transients in underground single core power cable configurations. The available approaches for the numerical evaluation of the infinite integrals and the corresponding assumptions and limitations are reported.

A novel numerical integration scheme, based on proper combinations of integration methods is proposed. The scheme has been applied successfully to a number of test cases, involving various cable configurations and earth resistivities over a wide frequency range from 1 Hz upto 10 MHz. The validity of the results obtained is justified using a suitable FEM formulation. It is shown that the assumptions implemented in the Electromagnetic Transients Program (EMTP) Cable constants/parameters supporting routines may lead to differences of 10–30%, and sometimes even more, compared to the results of the new method. The differences are noticeable above 10 kHz, except for the case of low earth resistivities, where differences are recorded even at power frequency. The new direct integration method shows a remarkable numerical stability and efficiency and does not suffer from the approximations implemented in other methods, which have been used for the evaluation of cable parameters to late. Therefore it may replace such methods in several popular software packages.

Application of the FEM in cases of underground cables in a two-layered earth gives results with significant differences from those obtained with the assumption of homogeneous earth. Differences start at less than 10% at power frequency and reach up to 20% at high frequencies. They also seem not to follow the penetration depth theory and cannot be disregarded. They justify the need for the further research into suitable mathematical models for the case of underground conductors in multilayered earth structures, as well as for efficient and general purpose methods for their numerical evaluation.

7 References

1 Carson, J.R.: 'Wave propagation in overhead wires with ground return', *Bell Syst. Tech. J.*, 1926, **5**, pp. 539–554
2 Pollaczek, F.: 'Ueber das Feld einer unendlich langen wechselstrom-durchflossenen Einfachleitung', *Elektr. Nachr. Tech.*, 1926, **3**, (4), pp. 339–359
3 Wedepohl, L.M., and Wilcox, D.J.: 'Transient analysis of underground power-transmission systems. System model and wave propagation characteristics,', *Proc. IEE.*, 1973, **120**, (2), pp. 253–260
4 Ametani, A.: 'A general formulation of impedance and admittance of cables', *IEEE Trans. Power Appar. Syst.*, 1980, **PAS-99**, (3), pp. 902–910
5 Dommel, H. W.: 'Electromagnetic Transients Program Reference Manual' (Bonneville Power Administration, Portland, OR, 1986)
6 Saad, O., Gaba, G., and Giroux, M.: 'A closed-form approximation for ground return impedance of underground cables', *IEEE Trans. Power Deliv.*, 1996, **PWRD-11**, (3), pp. 1536–1545
7 Nguen, T.T.: 'Earth return path impedances of underground cables – Pt. 1 Numerical integration of infinite integrals, Pt. 2 Evaluations using neural networks', *IEE Proc. Gener. Transm. Distrib.*, 1998, **145**, (6), pp. 621–633
8 Uribe, F. A., Naredo, J. L., Moreno, P., and Guardado, L.: 'Calculating earth return impedances for underground transmission cables'. Presented at IPST 2001 Conf., Rio de Janeiro, Brazil Available: http://www.ipst.org/IPST01Papers.htm, 2001
9 Sunde, E.D.: 'Earth conduction effects in transmission systems' (Dover Publications, 1968, 2nd edn.), pp. 99–139
10 Nakagawa, M., Ametani, A., and Iwamoto, K.: 'Further studies on wave propagation in overhead transmission lines with earth return: impedance of stratified earth', *Proc. IEE.*, 1973, **120**, (12), pp. 1521–1528
11 Yin, Y., and Dommel, H. W.: 'Calculation of frequency dependent impedances of underground power cables with finite element method', *IEEE Trans. Magn.*, 1989, **25**, (4), pp. 3025–3027
12 Papagiannis, G. K., Triantafyllidis, D. G., and Labridis, D. P.: 'A one-step finite element formulation for the modelling of single and double circuit transmission lines', *IEEE Trans. Power Syst.*, 2000, **15**, (1), pp. 33–38
13 Wedepohl, L.M., and Efthymiadis, A. E.: 'Wave propagation in transmission lines over lossy ground: a new, complete field solution', *Proc. IEE.*, 1978, **125**, (6), pp. 505–510
14 Perz, M.C., and Raghuveer, M.R.: 'Generalized derivation of fields and impedance correction factors of lossy transmission lines. Part II. Lossy conductors above lossy ground', *IEEE Trans. Power Appar. Syst.*, 1974, **PAS-93**, pp. 1832–1841
15 Davies, P., and Rabinowitch, P.: 'Methods of numerical integration' (Academic Press, 1984, 2nd edn.), pp. 104–223
16 Labridis, D., and Dokopoulos, P.: 'Finite element computation of field, losses and forces in a three-phase gas cable with non-symmetrical conductor arrangement', *IEEE Trans. Power Deliv.*, 1988, **PWRD-3**, (4), pp. 1326–1333
17 del Alamo, J. L.: 'A comparison among different techniques to achieve an optimum estimation of electrical grounding parameters in two-layered earth', *IEEE Trans. Power Deliv.*, 1993, **PWRD-8**, (4), pp. 1890–1899
18 Papagiannis, G., Tsiamitros, D., Labridis, D., and Dokopoulos, P.: 'Influence of earth stratification on overhead power transmission line impedances. A finite element approach'. Presented at MedPower 2002 Conf., Athens, Greece, 2002

8 Appendix

A new numerical integration technique is used for the calculation of the infinite integral of (6). It is based on combinations of numerical integration methods. Considering first the case where the horizontal distance x between the two conductors is not zero, the following procedure is applied.

The integral in (6) is divided into the following finite integrals:

$$\int_0^{a_1} \frac{e^{-(h+y)\sqrt{a^2+m^2}}}{a+\sqrt{a^2+m^2}} \cos(xa)da \tag{19}$$

$$\int_{a_1}^{a_2} \frac{e^{-(h+y)\sqrt{a^2+m^2}}}{a+\sqrt{a^2+m^2}} \cos(xa)da \tag{20}$$

$$\int_{a_i}^{a_{i+1}} \frac{e^{-(h+y)\sqrt{a^2+m^2}}}{a+\sqrt{a^2+m^2}} \cos(xa)da \tag{21}$$

$$\int_{a_6}^{a_7} \frac{e^{-(h+y)\sqrt{a^2+m^2}}}{a+\sqrt{a^2+m^2}} \cos(xa)da \tag{22}$$

$$\int_{\pi/2x}^{3\pi/2x} \frac{e^{-(h+y)\sqrt{a^2+m^2}}}{a+\sqrt{a^2+m^2}} \cos(xa)da \tag{23}$$

$$\int_{(2k+1)\pi/2x}^{(2k+3)\pi/2x} \frac{e^{-(h+y)\sqrt{a^2+m^2}}}{a+\sqrt{a^2+m^2}}\cos(xa)da \tag{24}$$

where $i=1, 2, \ldots, 6$, $\alpha_{i+1}=10*a_i$, $a_1=10^{-6}\frac{\pi}{2x}$, $a_7=\frac{\pi}{2x}$ and $k=0, 1, 2, 3, \ldots$. The integration limits of (19)–(22) result as the interval between zero and the first root of the cosine function is divided logarithmically. The shifted 16-point Gauss–Legendre method [15] is used to calculate (19)–(22). The above separation, in combination with the implemented integration method, can handle efficiently the initial steep descent of the integrand. For the calculation of (23) and (24), the 20-point shifted Lobatto rule [15] is applied, since this rule is best suited for the integration of periodic functions. The integrand is zero at the endpoints of the integration interval and this feature improves the accuracy of the method and minimises the computational time. The procedure stops when the absolute value of (24) for both the real and the imaginary part of the integral is less than a user defined tolerance, set to 10^{-9} for all applications in this paper.

If the horizontal distance x is zero, the integration procedure is different. The integral in (6) is again divided into the integrals (19)–(22), where now $a_1=10^{-6}\times 2\pi$ and $a_7=2\pi$ and it is calculated by the 16-point shifted Gauss–Legendre method. The rest integral until infinity is then transformed as:

$$\int_{a_7}^{\infty} \frac{e^{-(h+y)\sqrt{a^2+m^2}}}{a+\sqrt{a^2+m^2}}da = \int_{a_7}^{\infty} e^{-|h-y|a}\frac{e^{-(h+y)\sqrt{a^2+m^2}}e^{|h-y|a}}{a+\sqrt{a^2+m^2}}da = \int_{a_7}^{\infty} e^{-|h-y|a}\bar{g}(a)da \tag{25}$$

The 35-point shifted Gauss–Laguerre method [15] is used for the evaluation of (25), since it is the best method for the calculation of infinite integrals with exponential weight functions. The procedure is repeated iteratively. In each iteration, the use of the Gauss–Legendre method is extended by $2a_7$ intervals to the right of a_7 and the rest of the integral starting from $2a_7$ is calculated by the Gauss–Laguerre method. Convergence is achieved when the absolute difference between two succeeding values of the calculated integral is less than the predefined tolerance.

In all cases examined, convergence was achieved after 3–4 iterations.